ACS Synthetic Biology

Letter

pubs.acs.org/synthbio

GPCR-Based Chemical Biosensors for Medium-Chain Fatty Acids

Kuntal Mukherjee,[†] Souryadeep Bhattacharyya,[‡] and Pamela Peralta-Yahya*[,†,‡]

[†]School of Chemistry and Biochemistry, Georgia Institute of Technology, Atlanta, Georgia 30332, United States

[‡]School of Chemical and Biomolecular Engineering, Georgia Institute of Technology, Atlanta, Georgia 30332, United States

Supporting Information

ABSTRACT: A key limitation to engineering microbes for chemical production is a reliance on low-throughput chromatography-based screens for chemical detection. While colorimetric chemicals are amenable to high-throughput screens, many value-added chemicals are not colorimetric and require sensors for high-throughput screening. Here, we use G-protein coupled receptors (GPCRs) known to bind medium-chain fatty acids in mammalian cells to rapidly construct chemical sensors in yeast. Medium-chain fatty acids are immediate precursors to the advanced biofuel fatty acid methyl esters, which can serve as a "drop-in" replacement for D2 diesel. One of the sensors detects even-chain C8−C12 fatty acids with a 13- to 17-fold increase in signal after activation, with linear ranges up to 250 μM. Introduction of a synthetic response unit alters both dynamic and linear range, improving the sensor response to decanoic acid to a 30-fold increase in signal after activation, with a linear range up to 500 μM. To our knowledge, this is the first report of a whole-cell medium-chain fatty acid biosensor, which we envision could be applied to the evolutionary engineering of fatty acid-producing microbes. Given the affinity of GPCRs for a wide range of chemicals, it should be possible to rapidly assemble new biosensors by simply swapping the GPCR sensing unit. These sensors should be amenable to a variety of applications that require different dynamic and linear ranges, by introducing different response units.

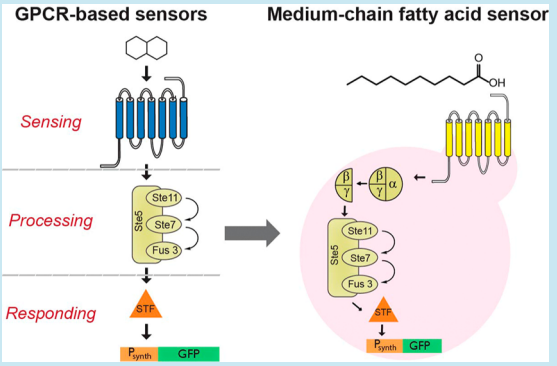

KEYWORDS: *chemical biosensors, biofuels, GPCR, yeast*

Identification of most microbially produced chemicals, including biofuels, currently relies on low-throughput (10^2 samples per day) chromatography-based screens due to the lack of a chemical handle that can be exploited for rapid colorimetric detection. Colorimetric microbially produced chemicals, such as lycopene and indigo, are amenable to high-throughput (10^7 samples per day) screening and have been successfully linked to genome engineering strategies for improved microbial production.[1,2] To make noncolorimetric chemicals similarly amenable to high-throughput screening, chemical sensors are needed, and, given the number of microbially produced chemicals of interest, these sensors should be capable of rapid assembly from existing biological parts. Most chemical biosensors, often encoded by RNA or protein, are composed of a single biological part with two distinct functional units physically linked to one another: a sensing unit to detect the chemical and an actuator unit to trigger a cellular process, such as protein fluorescence.[3] While single-part RNA-[3] and transcription factor-based[4] sensors have been applied to improve the microbial production of chemicals, fluorescence resonance energy transfer (FRET)-based sensors[5] and allosteric sensors[6] have not yet been applied to this problem. Efficiently transmitting chemical sensing information from the sensing unit to the actuator unit in single-part sensors is challenging, as the conformational change between these units must be extensively fine-tuned to effectively and efficiently transition between the on- and off states. This fine-tuning often requires a combination of *in vitro* and *in vivo* screening[7−12] to engineer a single-part sensor for each chemical of interest.

We reason that it will be more efficient to use two different biological parts to predictably and rapidly construct biosensors for user-specified chemicals: one part specialized in chemical sensing and another specialized in actuating, with information transmitted from the sensing unit to the actuating unit not *via* a physical linkage, but *via* an independent processing unit. Two-part chemical biosensors should overcome the need for extensive fine-tuning of each chemical sensor; all that would be needed is an array of known sensing units and an array of known actuator units that can be coupled to existing processing units to generate the desired chemical biosensor. Both histidine kinase receptors (HKRs)[13,14] and G-protein coupled receptors (GPCRs) exploit such sensing architecture by leveraging signal transduction pathways as processing units to relay the chemical sensing information from a receptor on the cell surface to the transcription factor actuator inside the cell. Unlike intracellular chemical sensors, HKRs and GPCRs detect chemicals non-invasively, on the outside of the cell. In the context of metabolic engineering, noninvasive chemical sensing will enable the construction of two-cell screening systems for the engineering of chemical-producing microbes (producer microbes). That is,

Received: December 17, 2014
Published: May 20, 2015

DOI: 10.1021/sb500365m
ACS Synth. Biol. 2015, 4, 1261−1269

after a producer microbe secretes the chemical of interest, a sensing microbe can detect the chemical in the culture medium. Advantages of such two-cell screening systems include the following: (1) the engineering of producer microbes without the cellular burden of also coding for the chemical sensor, (2) the application of genome engineering strategies to the producer microbe without detrimental effects to the sensor, (3) the implementation of strain improvement strategies to nongenetically tractable microbes for increased chemical production, and (4) the engineering of producer microbes for improved product secretion, which is not readily detectable by an intracellular sensor.

To rapidly construct chemical biosensors, we exploit GPCRs as the sensing unit because they naturally bind a wide variety of chemicals from biogenic amines and carbohydrates to lipids and odors.[15] GPCR-based chemical sensors have been previously engineered in the yeast *Saccharomyces cerevisiae*,[16−20] as this organism is amenable to heterologous GPCR expression.[21] Although in the 1990s and 2000s GPCRs were commonly coupled to the yeast mating pathway to discover new ligands for known GPCRs,[22,23] since then GPCR-based chemical sensing in yeast has been limited. Four main obstacles hindering GPCR-based sensing in yeast are (1) the difficult expression of functional heterologous GPCRs on the yeast cell surface,[24] (2) the unreliable coupling of heterologous GPCRs to the yeast mating pathway,[22,25] (3) the poor functional expression of mammalian olfactory GPCRs,[26] such that only two olfactory receptors (rat ORI7 and human OR17−40) have been functionally expressed in yeast[27] and have been used as the scaffold to express the ligand binding domain of other olfactory receptors (ORL829, ORL451, MOR226−1),[17] and (4) weak signal strength of the biosensor. We hypothesized that recent advances in synthetic biology, such as GPCR codon optimization, together with a large array of yeast promoters and plasmids, should overcome these obstacles and enable the rapid construction of GPCR-based chemical sensors in yeast. Specifically, using a plug-and-play strategy, sensing (GPCR), processing (signaling pathway) and response units (transcription factor/reporter gene) can be mixed and matched to predictably generate chemical sensors (Figure 1).

Here, we report the rapid construction of GPCR-based yeast sensors to detect saturated medium-chain fatty acids. Fatty acids are the immediate precursors to the advanced biofuel fatty acid methyl esters (FAMEs), which can serve as a "drop in" replacement for D2 diesel.[28] FAMEs derived from medium-chain fatty acids (C8−C12) have better cold properties than traditional canola oil-derived (C16−C22) FAMEs.[29,30] Microbial production of medium-chain fatty acids is a challenging problem both in *S. cerevisiae*[31] and *Escherichia coli*,[32,33] with titers reaching less than 100 mg/L, a stark contrast to the titers reached for C16−C18 in *E. coli* (5 g/L)[34] and *S. cerevisiae* (400 mg/L).[35] A medium-chain fatty acid sensor could be used, in the future, for the engineering of microbes with improved medium-chain fatty acid production. In this work, we first determined the signal after activation of the endogenous Ste2/α-factor sensor to determine the upper limit for future GPCR-based chemical sensors that would rely on heterologous GPCR sensing units coupling to the yeast mating pathway. Then, we coupled two GPCRs known to bind fatty acids in mammalian cells to the yeast mating pathway. One of the GPCR-based sensors reliably detects C8−C12 fatty acids with a 13- to 17-fold increase in signal after activation. The sensor is specific to medium-chain fatty acids, not being able to detect long-chain

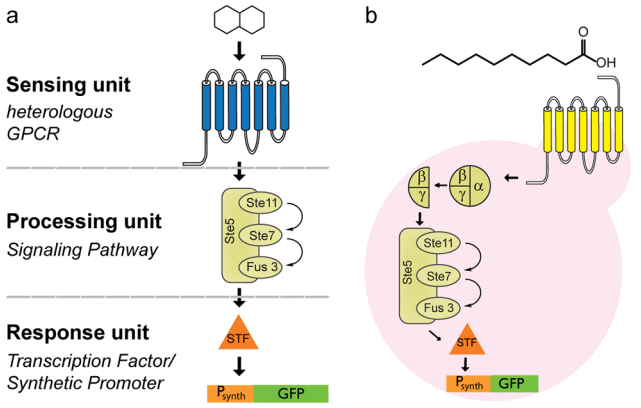

Figure 1. GPCR-based chemical biosensor. (a) GPCR-based chemical sensors can be rapidly assembled from existing biological parts. GPCRs are used as sensing units to detect chemicals in the culture medium (hexagons). Signaling pathways are used as processing units to transmit a chemical signal from the sensing to the response unit. The response unit, composed of a transcription factor and a synthetic promoter (P_{synth}), activates transcription of a reporter gene, such as green fluorescent protein (GFP). (b) Medium-chain fatty acid biosensor. A heterologous GPCR (yellow) detects a medium-chain fatty acid in the culture medium, transmits this chemical signal to the yeast mating-pathway (green), which relays it to a synthetic transcription factor (STF, orange). The STF activates transcription of GFP.

fatty acids or medium-chain aldehydes, alcohols or C10 esters. Next, we improved the biosensor features by introducing a synthetic response unit capable of taking information from the yeast mating pathway and exclusively activating green fluorescent protein (GFP) expression, resulting in a decanoic acid sensor with a 30-fold increase in signal after activation. Introduction of the synthetic response unit also altered the linear range of the sensor. Finally, we determined the linear and dynamic range of the sensors to assess their utility in chemical screening applications. To our knowledge, this is the first report of a whole-cell biosensor for medium-chain fatty acids and the first coupling of a synthetic response unit to a GPCR-based yeast sensor for the sensing of nonendogenous chemicals. The rapid generation of noninvasive chemical sensors such as the ones presented in this work will be critical to the future engineering of chemical-producing microbes (Table 1).

To engineer a GPCR-based chemical sensor strain, we deleted two genes in the yeast mating pathway, to avoid cell cycle arrest (*far1*) and reduce the spontaneous rate of GPCR inactivation upon chemical sensing (*sst2*).[36,37] Next, we determined the dynamic range of the endogenous GPCR-based sensor (Ste2/α-factor) using the mating pathway-dependent transcription factor Ste12, which upregulates mating pathway genes (Figure 2a). We tested the response of the Ste2/α-factor sensor using GFP under control of two mating pathway promoters (P_{Fus1} and P_{Fig1}) from either a single-copy (s) or a multicopy (m) reporter plasmids (Figure 2b).[19,38] The maximum x-fold increase in signal after activation, defined as the maximal GFP fluorescence in the presence of chemical over the signal in the absence of chemical, for P_{Fus1} and P_{Fig1} from a multicopy plasmid was 24- and 68-fold, respectively (difference between increases statistically significant, P-value 0.01) (Figure 2c). The maximum x-fold increase in signal after activation for P_{Fus1} and P_{Fig1} from a single-copy plasmid was 20- and 40-fold, respectively (difference between increases statistically signifi-

DOI: 10.1021/sb500365m
ACS Synth. Biol. 2015, 4, 1261−1269

Table 1. Strains Used in This Study

strain	genotype
PPY11	W303: MATa, leu2−3, trp1−1, can1−100, ura3−1, ade2−1, his3−11
PPY62	PPY11 Δ*far1*
PPY58	PPY11 Δ*far1*, Δ*sst2*
PPY140	PPY11 Δ*far1*, Δ*sst2*, Δ*ste2*
PPY161	PPY11 Δ*far1*, Δ*sst2*, Δ*ste2*, Δ*ste12*
PPY638	PPY58, pESC-Leu2-P_{Fus1}-GFP
PPY639	PPY58, pESC-Leu2-P_{Fig1}-GFP
PPY640	PPY58, pRS415-Leu2-P_{Fus1}-GFP
PPY641	PPY58, pRS415-Leu2-P_{Fig1}-GFP
PPY653	PPY58, pESC-Leu2
PPY654	PPY58, pRS415-Leu2
PPY643	PPY140, pESC-His3-P_{TEF1}-OR1G1, pRS415-Leu2-P_{Fig1}-GFP
PPY644	PPY140, pESC-His3-P_{TEF1}-GPR40, pRS415-Leu2-P_{Fig1}-GFP
PPY912	PPY140, pRS13-His3-P_{TEF1}-OR1G1, pRS415-Leu2-P_{Fig1}-GFP
PPY913	PPY140, pESC-His3-P_{TEF1}-OR1G1-P_{ADH1}-G_{olf}, pRS415-Leu2-P_{Fig1}-GFP
PPY914	PPY140, pESC-His3-P_{TEF1}-OR1G1-P_{ADH1}-GPA1-G_{olf}, pRS415-Leu2-P_{Fig1}-GFP
PPY915	PPY140, pRS13-His3-P_{TEF1}-OR1G1-P_{ADH1}-GPA1-G_{olf}, pRS415-Leu2-P_{Fig1}-GFP
PPY656	PPY140, pESC-His3, pRS415-Leu2
PPY916	PPY140, pRS13-His3, pRS415-Leu2
PPY794	PPY140, pESC-His3, pRS415-Leu2-P_{Fig1}-GFP
PPY795	PPY161, pESC-His3-P_{TEF1}-OR1G1, pRS415-Leu2-P_{Fig1}-GFP
PPY832	PPY161, pESC-His3-P_{TEF1}-GPR40, pRS415-Leu2-P_{Fig1}-GFP
PPY657	PPY161, pESC-His3, pESC-Leu2
PPY833	PPY161, pESC-His3, pRS415-Leu2-P_{Fig1}-GFP
PPY661	PPY161, pESC-His3-P_{TEF1}-OR1G1-P_{ADH1}-STF1, pESC-Leu2-$P_{Gal4(5x)}$-GFP
PPY818	PPY161, pESC-His3-P_{TEF1}-OR1G1-P_{ADH1}-STF2, pESC-Leu2-$P_{LexA(4x)}$-GFP
PPY796	PPY161, pESC-His3-P_{TEF1}-GPR40-P_{ADH1}-STF1, pESC-Leu2, $P_{Gal4(5x)}$-GFP
PPY819	PPY161, pESC-His3-P_{TEF1}-GPR40-P_{ADH1}-STF2, pESC-Leu2-$P_{LexA(4x)}$-GFP

cant, *P*-value 0.01). The difference in maximum *x*-fold increase in signal activation between P_{Fig1}-GFP (s) and P_{Fig1}-GFP(m) was statistically significant (*P*-value 0.01).

To generate a sensor to detect medium-chain fatty acids, we replaced the endogenous GPCR Ste2 with a GPCR known to bind medium-chain fatty acids in mammalian cells and coupled it to the yeast mating pathway with P_{Fig1}-GFP as the reporter plasmid, resulting in GFP fluorescence upon medium-chain fatty acid addition (Figure 2d). We tested the olfactory receptor OR1G1[39] and the free fatty acid receptor GPR40.[40] First, we tested OR1G1 and GPR40 sensing of even, medium-chain saturated fatty acids (C8−C16) using P_{Fig1}-GFP(m), however, we did not see any reliable signal after fatty acid addition (Figure S1). Hypothesizing that the large standard deviation of P_{Fig1}-GFP(m) contributed to the inability to detect medium-chain fatty acids, we tested P_{Fig1}-GFP(s) as the reporter plasmid. Using P_{Fig1}-GFP(s) enabled the OR1G1-based sensor to detect C8, C10 and C12 fatty acids with 13-, 17-, and 13-fold increases in signal after activation, respectively (Figure 2e,f). Using P_{Fig1}-GFP(s) also enabled the GPR40-based sensor to detect C8, C10 and C12 saturated fatty acids, with 14-, 25-, and 16-fold increases in signal after activation, respectively (Figure 2g,h). The noisiness of the GPR40-based sensor dose response curves, however, suggests that this sensor may be unreliable. Neither the OR1G1- nor the GPR40-based sensors detected C14 or C16 saturated fatty acids, which precipitate out of solution at 250 μM. We explored whether the OR1G1-based sensor signal could be improved by expressing OR1G1 from a single-copy (s) rather than a multicopy (m) plasmid. OR1G1(m) and OR1G1(s) resulted in similar increases in signal after activation with 500 μM decanoic acid; however, the OR1G1(s) dose response curve was unreliable (Figure S2a). We also attempted to improve the OR1G1-based sensor signal by using (i) the mammalian olfactory G_α subunit (G_{olf}) that normally couples to OR1G1 instead of the yeast G_α (GPA1), and (ii) a hybrid G_α subunit composed of GPA1 carrying the five C-terminal amino acids from G_{olf}, both strategies having been previously successful to link GPCR sensing to the yeast mating pathway.[19,36,37,41] Surprisingly, G_α subunit engineering did not improve the OR1G1-based sensor signal. Using the chromosomal GPA1 had the highest increase in signal after activation above 250 μM decanoic acid (Figure S2b).

To confirm that the medium-chain fatty acids were signaling *via* the GPCR sensing unit and not through a different cellular mechanism, we tested the chemical sensor strain in the presence and absence of the GPCRs and either 0 or 500 μM decanoic acid. An increase in GFP fluorescence was only observed in the presence of both 500 μM decanoic acid and either OR1G1 (*P*-value <0.0001) or GPR40 (*P*-value <0.0001) (Figure 3b). To show that the chemical signal was transmitted *via* the yeast mating pathway, we deleted the mating pathway transcription factor Ste12. We then tested the sensor strain in the presence and absence of the GPCRs and either 0 or 500 μM decanoic acid. There was no increase in GFP fluorescence in the absence of Ste12 and the presence of both GPCR and 500 μM decanoic acid (Figure 3c). Interestingly, deletion of Ste12 results in higher overall GFP background fluorescence, which we attribute to transcription factors other than Ste12, such as the TATA box binding protein, binding to the pheromone response elements in P_{Fig1}-GFP(s). Taken together, these data demonstrate that decanoic acid is sensed by the heterologous GPCR, which uses the yeast mating pathway as the processing unit and not a different cellular mechanism.

To determine the specificity of the OR1G1- and the GPR40-based sensors, we tested their detection of saturated C8, C10 and C12 fatty aldehydes, important targets for the perfume industry, and saturated C8, C10 and C12 fatty alcohols, important targets for the detergent industry, as well as C10 fatty acid methyl- and ethyl-esters, which are advanced biofuels that can serve as replacements for D2 diesel (Figure 3d,e). Except for C10 aldehyde, the OR1G1-based sensor was unable to detect aldehydes, alcohols or esters with more than a 3-fold increase in signal after activation. The GPR40-based sensor detected the C10 aldehyde at 125 μM and the C12 aldehyde at 250 μM, both with a 3-fold increase in signal after activation, but was unable to detect the C8 aldehyde. Similarly to the OR1G1-based sensor, the GPR40-based sensor was unable to detect alcohols or esters with more than a 3-fold increase in signal after activation. These data show that the OR1G1- and GPR40-based sensors are specific to medium chain fatty acids.

To improve the biosensor response to medium-chain fatty acids, we bypassed the endogenous mating pathway transcription factor Ste12, which activates more than 100 mating pathway genes.[42] To engineer a system in which medium-chain fatty acid sensing would trigger only GFP transcription, we replaced Ste12 with one of two synthetic transcription factors (STFs): (1) STF1, which is composed of the Ste12 phosphorylation domain and the Gal4 activation and DNA

DOI: 10.1021/sb500365m
ACS Synth. Biol. 2015, 4, 1261−1269

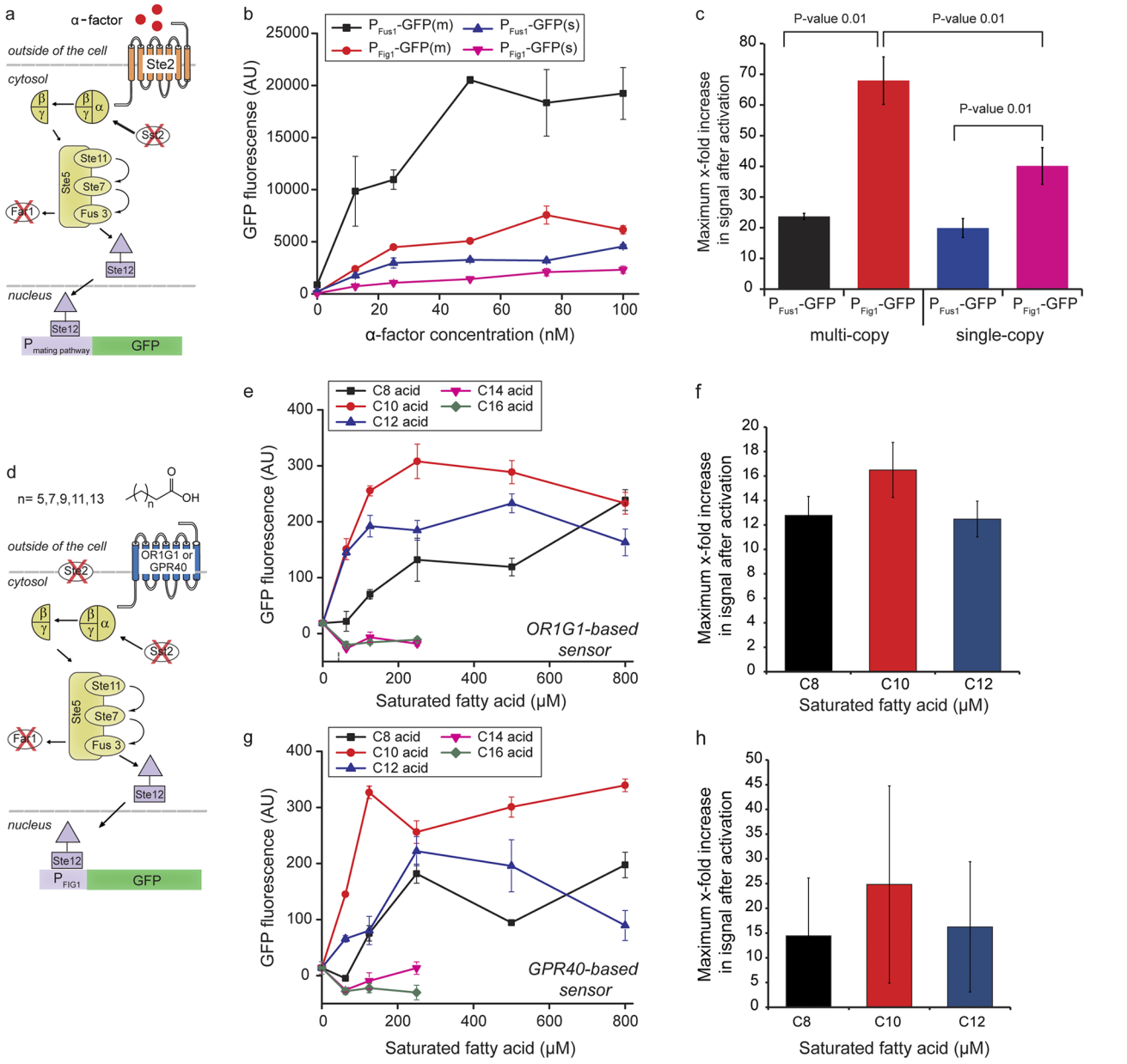

Figure 2. GPCR-based sensors. (a) Ste2/α-factor sensor schematic. The Ste2 GPCR (orange) detects α-factor in the culture medium, the chemical signal is transmitted *via* the yeast mating pathway (green) to the mating pathway transcription factor Ste12 (purple). Ste12 activates transcription of green fluorescent protein (GFP) under control of a mating pathway promoter ($P_{mating\ pathway}$). The GPCR-based chemical sensor strain has the *far1* and *sst2* genes deleted to avoid cell cycle arrest and to reduce the spontaneous rate of GPCR inactivation upon chemical sensing, respectively. (b) Ste2/α-factor sensor dose response curves carrying GFP under control of two mating pathway promoters (P_{Fus1} and P_{Fig1}) from either a single-copy (s) or a multicopy (m) reporter plasmids. (c) Maximum *x*-fold increase in signal after activation: P_{Fus1}-GFP(m): 50 nM α-factor, P_{Fig1}-GFP(m): 75 nM α-factor, P_{Fus1}-GFP(s) and P_{Fig1}-GFP(s): 100 nM α-factor. *P*-values, obtained from a two-tailed *t* test, shown for statistically different samples. (d) Medium-chain fatty acid sensor schematic. Either the OR1G1 or GPR40 GPCR (blue) detects medium-chain fatty acids in the culture medium, the chemical signal is transmitted *via* the yeast mating pathway (green) to the mating pathway transcription factor Ste12 (purple). Ste12 activates transcription of GFP under control of the P_{Fig1} promoter. In addition to deletion of the *far1*and *sst2* genes, the medium-chain fatty acid sensor strain has the endogenous GPCR Ste2 deleted (W303 Δ*far1*, Δ*sst2*, Δ*ste2*). (e) Dose response curves for the OR1G1-based sensor (PPY643) with C8, C10, C12, C14 and C16 acids. (f) OR1G1-based sensor maximum *x*-fold increase in signal after activation with C8 (800 μM), C10 (250 μM) and C12 (500 μM) acids. (g) Dose response curves for the GPR40-based sensor (PPY644) with C8, C10, C12, C14 and C16 acids. (h) GPR40-based sensor maximum *x*-fold increase in signal after activation with C8 (800 μM), C10 (800 μM) and C12 (250 μM) acids. For f and h, none of the samples showed statistical difference using a two-tailed *t* test. All experiments were done in triplicate and the error bars represent the standard deviation from the mean.

binding domains,[43] and (2) STF2, which is composed of the Ste12 phosphorylation domain, the synthetic B42 activation domain and the bacterial LexA DNA binding domain.[44,45] STF1 activates transcription of GFP placed under control of a synthetic minimal promoter carrying five Gal4 DNA binding sites ($P_{Gal4(5x)}$). STF2 activates transcription of GFP placed under control of a synthetic minimal promoter carrying four lexA DNA binding sites ($P_{LexA(4x)}$) (Figure 4a,b). Under glucose conditions, STF1 triggers only $P_{Gal4(5x)}$-GFP expression as endogenous galactose promoters are repressed by Mig1.[46]

DOI: 10.1021/sb500365m
ACS Synth. Biol. 2015, 4, 1261−1269

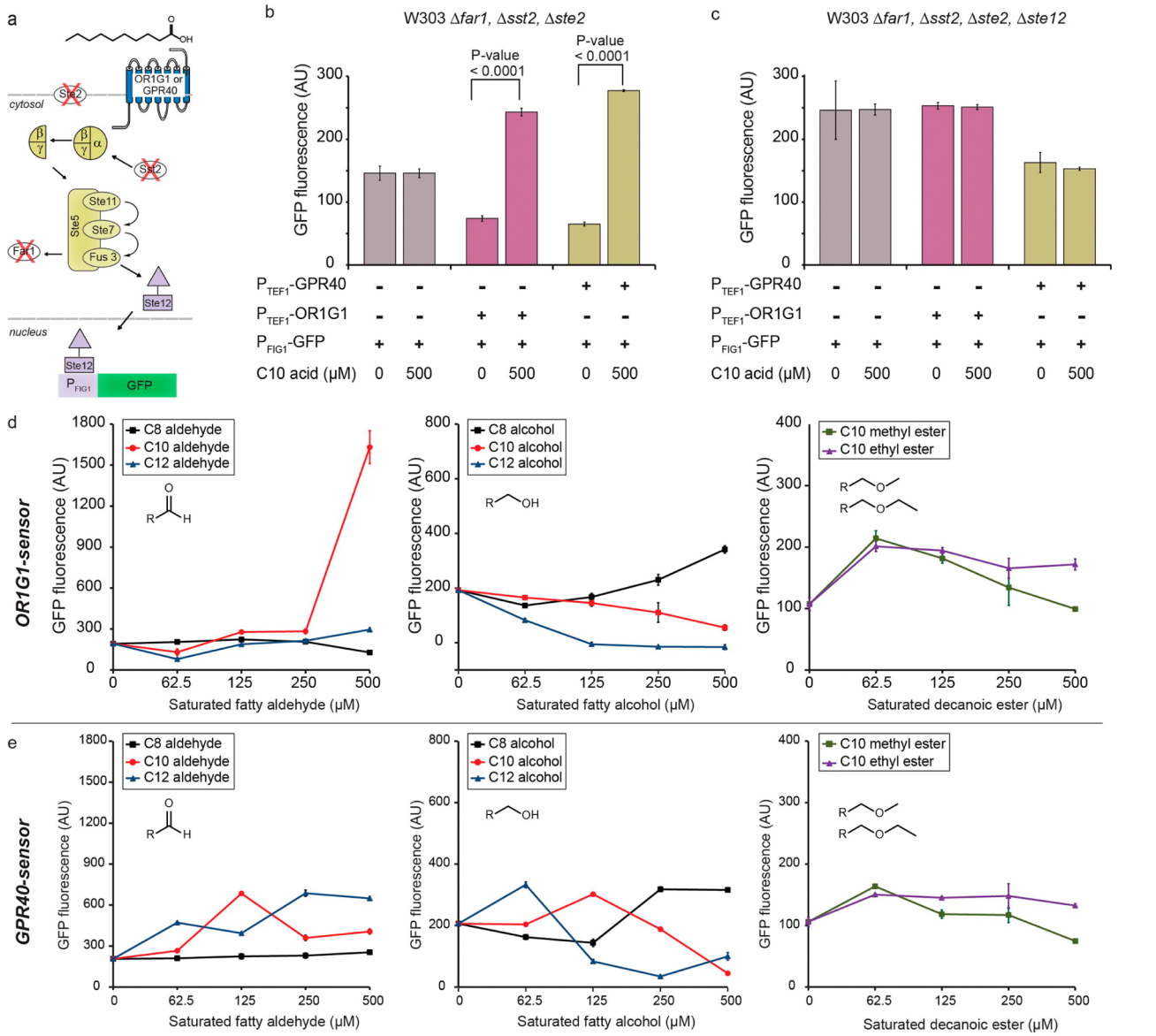

Figure 3. GPCR-based sensors signal routing and GPCR-based sensor response to fatty aldehydes, alcohols, and esters. (a) GPCR-based sensor schematic: chemical sensor strain (W303 Δ*far1*, Δ*sst2*, Δ*ste2*) expressing either OR1G1 or GPR40 carrying P_{Fig1}-GFP(s) as the reporter plasmid. (b) GPCR-based sensor signal requires sensing unit (GPCR) for chemical sensing. Chemical sensor strain expressing no GPCR, OR1G1 or GPR40 in the presence of 0 or 500 μM decanoic (C10) acid using P_{Fig1}-GFP(s) as the reporter plasmid. (c) GPCR-based sensor signal requires response unit (Ste12) for chemical sensing. Chemical sensor strain with endogenous yeast mating pathway transcription factor Ste12 deleted (W303 Δ*far1*, Δ*sst2*, Δ*ste2*, Δ*ste12*) expressing no GPCR, OR1G1 or GPR40 in the presence of 0 or 500 μM decanoic (C10) acid using P_{Fig1}-GFP(s) as the reporter plasmid. *P*-values, obtained from a two-tailed *t* test, shown for statistically different samples. (d) Dose response curves for the OR1G1-based sensor and (e) GPR40-based sensor with C8, C10 and C12 fatty aldehydes, alcohols and C10 methyl- and ethyl-esters. All experiments were done in triplicate and the error bars represent the standard deviation from the mean.

STF2 triggers only expression of $P_{LexA(4x)}$-GFP as lexA binding sites are of prokaryotic origin and orthogonal to the yeast machinery. Coupling of the STF1/$P_{Gal4(5x)}$-GFP response unit to the OR1G1-based sensor resulted in a 30-fold increase in signal after activation in the presence of 800 μM decanoic acid (Figure 4c,d), which is almost a 200% improvement over the Ste12/P_{Fig1}-GFP(s) response unit. Further, the OR1G1-based sensor coupled to the STF1/$P_{Gal4(5x)}$-GFP response unit also had an improved linear range, reaching to 500 μM decanoic acid when compared to the OR1G1-based sensor coupled to the Ste12/P_{Fig1}-GFP(s) response unit, in which linear range plateaued at 250 μM decanoic acid. Coupling of the STF2/$P_{LexA(4x)}$-GFP response unit to the OR1G1-based sensor resulted in only a 7-fold increase in signal after activation in the presence of 800 μM decanoic acid. Coupling of the STF1/$P_{Gal4(5x)}$-GFP response unit to the GPR40-based sensor unit resulted in a 28-fold increase in signal after activation in the presence of 500 μM decanoic acid (Figure 4e,f), though this increase was not statistically significant when compared to coupling the Ste12/P_{Fig1}-GFP(s) response unit to the GPR40-based sensor (25-fold increase). Coupling the GPR40-based sensor to STF2/$P_{LexA(4x)}$ showed only a 4-fold increase in GFP expression upon decanoic acid exposure.

We determined the utility of the GPCR-based sensors for medium-chain fatty acid screening applications by measuring the biosensor features, including dynamic and linear range,

DOI: 10.1021/sb500365m
ACS Synth. Biol. 2015, 4, 1261−1269

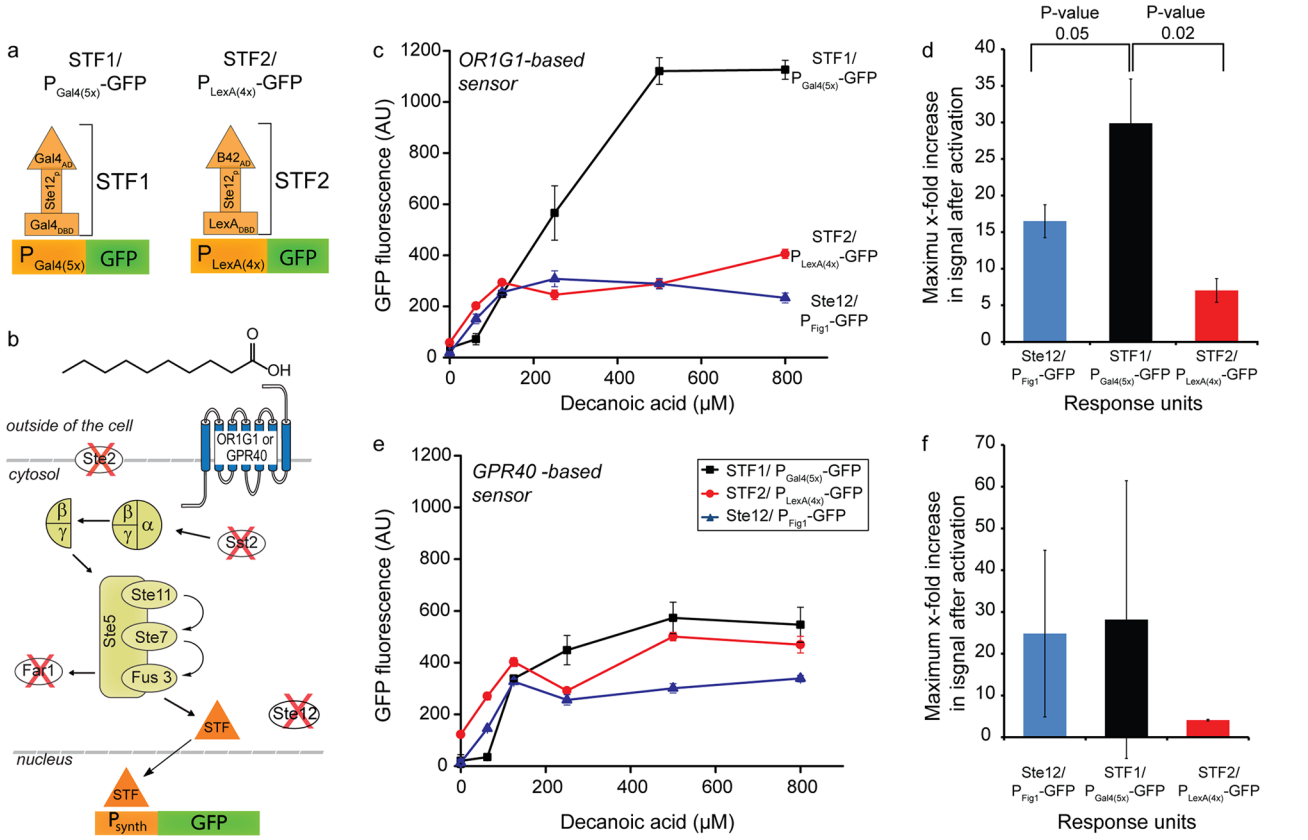

Figure 4. GPCR-based sensors with synthetic response units. (a) Synthetic transcription factor (STF)/synthetic promoter composition. AD = activation domain, P = phosphorylation domain, DBD = DNA binding domain. STF1 is composed of a $Gal4_{AD}$, $Ste12_p$ and a $Gal4_{DBD}$. STF1 binds to $P_{Gal4(5x)}$, a synthetic promoter carrying five Gal4 DNA binding sites. STF2 is composed of a $B42_{AD}$, $Ste12_p$ and a $LexA_{DBD}$. STF2 binds to $P_{LexA(4x)}$, a synthetic promoter carrying four lexA DNA binding sites. (b) Schematic of the OR1G1- and GPR40-based sensors using a synthetic response unit ($STF/P_{synthetic}$-GFP). In addition to deletion of the *far1*, *sst2*, and *ste2* genes, the chemical sensor strain using a synthetic response unit also has the endogenous transcription factor Ste12 deleted (W303 Δ*far1*, Δ*sst2*, Δ*ste2*, Δ*ste12*). (c) Dose response curves for decanoic acid using the OR1G1-based sensor coupled to $Ste12/P_{Fig1}$-GFP(s) (blue), $STF1/P_{Gal4(5x)}$-GFP (black), or $STF2/P_{LexA(4x)}$-GFP (red) response units. (d) OR1G1-based sensor maximum *x*-fold increase in signal after activation upon addition of decanoic acid when coupled to $Ste12/P_{Fig1}$-GFP(s): 250 μM C10 acid, $STF1/P_{Gal4(5x)}$-GFP: 800 μM C10 acid, and $STF2/P_{LexA(4x)}$-GFP: 800 μM C10 acid. (e) Dose response curves for decanoic acid using the GPR40-based sensor coupled to $Ste12/P_{Fig1}$-GFP(s) (blue), $STF1/P_{Gal4(5x)}$-GFP (black) or $STF2/P_{LexA(4x)}$-GFP (red) response units. (f) GPR40-based sensor maximum *x*-fold increase in signal after activation upon addition of decanoic acid when coupled to $Ste12/P_{Fig1}$-GFP(s): 800 μM C10 acid, $STF1/P_{Gal4(5x)}$-GFP: 500 μM C10 acid, and $STF2/P_{LexA(4x)}$-GFP: 500 μM C10 acid. *P*-values, obtained from a two-tailed *t* test, shown for statistically different samples. All experiments were done in triplicate and the error bars represent the standard deviation from the mean.

binding affinity and sensitivity.[4] Dose response curves of the GPCR-based sensors in the presence of fatty acids were fitted to the Hill equation (Table 2). Response curves for the OR1G1- and GPR40-based sensors could be fitted to transfer functions for all saturated fatty acids. For the detection of decanoic acid with the OR1G1-based sensor, changing the response unit from $Ste12/P_{Fig1}$-GFP(s) to $STF1/P_{Gal4(5x)}$-GFP not only improved the dynamic range from a 17- to a 30-fold increase, but also changed the linear range from 34−250 to 110−500 μM and increased the K_M from 65 to 248 μM. Further, the sensitivity of the response to decanoic acid was also increased from n = 2.3 to n = 3.2. For the detection of decanoic acid with the GPR40-based sensor, changing the response unit from $Ste12/P_{Fig1}$-GFP(s) to $STF1/P_{Gal4(5x)}$-GFP did not result in a statistically significant change in dynamic range, but changed the linear range from 36−100 to 47−250 μM and increased the K_M from 69 to 114 μM. Therefore, by simply changing the response unit, the dynamic and linear range of GPCR-based sensors can be altered without the need for using a GPCR with a different binding affinity for the compound of interest. Sensors with different dynamic and linear ranges may be useful to different applications.

Here, we show that advances in synthetic biology enable the rapid assembly of GPCR-based yeast biosensors for the detection of chemicals. Our proof-of-principle medium-chain fatty acid sensors have up to a 30-fold increase in signal after activation in the presence of decanoic acid and are specific to medium-chain fatty acids over same chain-length aldehydes, alcohols, and C10 methyl- and ethyl esters. We envision that GPCR-based biosensors may be used for similarly specific sensing of other target chemicals, by simply swapping the GPCR sensing unit. We have shown that the signal through the sensor can be rerouted and, more importantly, that the biosensor features, such as dynamic and linear range, binding affinity and sensitivity can be altered by using different response units. Altering the biosensor features without resorting to new GPCR sensing units increases the utility of GPCR-based sensors. We envision that different applications will require sensors with different features; for example, the engineering of microbes for the production of medium-chain fatty acids will require sensors with different linear ranges as the engineering

DOI: 10.1021/sb500365m
ACS Synth. Biol. 2015, 4, 1261−1269

Table 2. Biosensor Performance Features[a]

background strain	reporter plasmid	GPCR	TF	chemical	GFP max (AU)	dynamic range	linear range	K_M (μM)	Hill coeff. (n)
W303 Δ*far1*, Δ*sst2*	P_{Fig1}-GFP(s)	Ste2	Ste12	α factor	2314	40	8−50nM	0.03	1.7
	P_{Fus1}-GFP(s)	Ste2	Ste12	α factor	4565	20	2−25nM	0.02	1.1
	P_{Fus1}-GFP(m)	Ste2	Ste12	α factor	20525	24	5−25nM	0.02	1.8
	P_{Fig1}-GFP(m)	Ste2	Ste12	α factor	7566	68	4−25nM	0.02	1.4
W303 Δ*far1*, Δ*sst2* Δste2	P_{Fig1}-GFP(s)	OR1G1	Ste12	C8 acid	239	13	19−250 μM	230	1.5
		OR1G1	Ste12	C10 acid	308	17	34−250 μM	65	2.25
		OR1G1	Ste12	C12 acid	233	13	1−250 μM	50	0.85
	P_{Fig1}-GFP(s)	GPR40	Ste12	C8 acid	197	14	36−250 μM	162	2.25
		GPR40	Ste12	C10 acid	339	25	36−100 μM	69	4.1
		GPR40	Ste12	C12 acid	222	16	2−250 μM	148	0.7
W303 Δ*far1*, Δ*sst2*, Δ*ste2*, Δ*ste12*	$P_{Gal4(5x)}$- GFP(m)	OR1G1	STF1	C10 acid	1126	30	110−500 μM	248	3.2
		GPR40	STF1	C10 acid	573	28	47−250 μM	114	3
	$P_{LexA(4x)}$-GFP(m)	OR1G1	STF2	C10 acid	405	7	2−100 μM	69	0.62
		GPR40	STF2	C10 acid	501	4	4−100 μM	62	0.77

[a]Dose response curves were fitted to the Hill equation to derive the biosensor transfer functions from which the performance features were obtained. TF: transcription factor. GFP_{max} is the highest fluorescence obtained by the sensor in the presence *vs* the absence of the chemical. Dynamic range is the ratio of the highest fluorescence obtained by the sensor in the presence *vs* the absence of the chemical. Linear range is the series of chemical concentrations for which a change in signal can be detected by the sensor. The minimum limit of the linear range is estimated as the chemical concentration corresponding to 10% signal saturation from the fitted model. K_M is the chemical concentration at half maximal signal, estimated by linear interpolation from experimental data. Hill coefficient (n) is the sensitivity of the system.

progresses. In this work, we have shown that we can change the linear range from 34−250 to 110−500 μM decanoic acid by simply swapping the response unit. As both the sensing and response units can be swapped into and out of the system to alter chemical target and biosensor features, respectively, we can rapidly construct sensors for user-specified chemicals.

GPCR-based yeast sensors detect chemicals on the outside of the cell, and thus can only detect compounds secreted from producer cells. Therefore, GPCR-based sensors will need to detect medium-chain fatty acids, such as decanoic acid, in a mixture of other secreted acids. At this point, the OR1G1-based sensor cannot detect decanoic acid in a mixture with C14 and C16 acids (Figure S3), which we believe is partially due to the toxicity of fatty acids to cell growth (Figure S4). Further, not all chemicals are secreted from cells, such as charged (*e.g.*, phosphorylated chemicals) or very large compounds (*e.g.*, triacylglycerides), and these compounds will require an intracellular chemical sensor. Nevertheless, from a microbial chemical production perspective, it is advantageous to secrete the chemical of interest or engineer microbes to do so, as chemical secretion allows for continuous culture and compound extraction, thus removing the cost associated with cell breakage and compound extraction.

Transforming decanoic acid concentration to titers, the OR1G1-based sensor coupled to the Ste12/P_{Fig1}-GFP(s) response unit can detect decanoic acid titers from 6 to 43 mg/L while the OR1G1-based sensor coupled to the STF1/$P_{Gal4(5x)}$-GFP response unit can detect decanoic acid titers from 19 to 86 mg/L. Since extracellular decanoic acid production in *E. coli* is ∼80 mg/L[33] and *S. cerevisiae*'s is ∼3 mg/L[31] the OR1G1-based sensor has the appropriate linear range to screen for decanoic acid-producing microbes with increased titers. In another application, the sensors can be used as a systems biology tool to interrogate less engineered strains for alternative routes to increase fatty acid production in a medium-throughput fashion (10^3 samples/day). Such a throughput would allow the screening of entire transposon libraries, or simply existing microbial deletion collections, such as those from *S. cerevisiae*[47] or *E. coli*[48] for the discovery of novel regulatory elements that affect the decanoic acid production.

METHODS

Biosensing Protocol. For the Ste2/α-factor sensor, strains PPY638, PPY639, PPY640, PPY641 were grown overnight in synthetic complete media with 2% glucose and lacking leucine (SD glu (L^-)). The next day, the cells were used to inoculate 20 mL of SD glu (L^-) to an OD_{600} = 0.06 and incubated for 18 h at 30 °C (150 r.p.m.). The cells were centrifuged, resuspended in 5 mL SD glu (L^-), and used to inoculate 5 mL of fresh SD glu (L^-) to OD_{600} = 0.6. α-factor (0−100 nM, Zymo Y1001) was added to the medium and incubated for 4 h at 30 °C (150 r.p.m.) before reading for cell fluorescence using a flow cytometer. For the OR1G1- and GPR40-based sensors using Ste12/P_{Fig1}-GFP response unit, strains PPY643, PPY644 were grown overnight in SD glu and lacking histidine and leucine (SD glu (HL^-)). The next day, the cells were used to inoculate 20 mL of SD glu (HL^-) to an OD_{600} = 0.06 and incubated for 18 h at 15 °C (150 r.p.m.). The cells were centrifuged, resuspended in 2 mL SD glu (HL^-), and used to innoculate 5 mL of fresh SD glu (HL^-) to OD_{600} = 0.6. C8, C10, C12, C14 and C16 saturated fatty acids (0−800 μM) were added to the medium and incubated for 4 h at 30 °C (150 r.p.m.) before reading for cell fluorescence using a flow cytometer. For the OR1G1-based sensor expressed from a single copy plasmid, and when coupled to G_{olf} and GPA1-G_{olf}, strains PPY912, PPY913, PPY914, and PPY915 were processed using the same protocol as the OR1G1-based sensor using Ste12/P_{Fig1}-GFP response unit. For the OR1G1- and GPR40-based sensors with synthetic response units, strains PPY661, PPY796, PPY818, PPY819, were processed using the same protocol as the OR1G1- and GPR40-based sensors using the Ste12/P_{Fig1}-GFP response unit. All fatty acids were dissolved in DMSO and the final concentration of DMSO in the cultures was 1%. GFP fluorescence was measured using a BD LSRII flow cytometer with the following settings: 488 nM laser line, 515−545 nm filter, FSC: 178 V, SSC: 122 V, FITC: 600 V.

DOI: 10.1021/sb500365m
ACS Synth. Biol. 2015, 4, 1261−1269

Fluorescence data was collected from 10,000 viable cells for each experiment. Flow cytometry histogram analysis was done using FlowJo software.

Statistical Analysis. For all experiments, cell autofluorescence, measured using the biosensor strain with empty plasmids, was subtracted from the fluorescence of the biosensor at all chemical concentrations to obtain GFP fluorescence attributable to the sensor. x-fold increase in signal after activation is defined as the quotient of GFP fluorescence in the presence and absence (0 μM) of the chemical. Standard deviation for the x-fold increase in GFP fluorescence was calculated using

$$\Delta z = z\mathrm{SQRT}[(\Delta x/x)^2 + (\Delta y/y)^2]$$

where x and Δx are the average fluorescence and standard deviation in the absence of the chemical, respectively; y and Δy are the average fluorescence and standard deviation in the presence of the chemical, respectively; and z and Δz are x-fold increase in signal activation and its standard deviation, respectively.

Biosensor Performance Calculations. The Hill equation was used to fit the transfer function to derive the biosensor performance features:

$$\mathrm{GFP} = \mathrm{GFP}_0 + (\mathrm{GFP}_{\mathrm{chemical}} - \mathrm{GFP}_0)(x^n/{K_\mathrm{M}}^n + x^n)$$

where GFP_0 is the fluorescence in the absence of chemical, $\mathrm{GFP}_{\mathrm{chemical}}$ is the fluorescence in the presence of the chemical, x is the ligand concentration, K_M is the ligand concentration that results in half-maximal signal, and n is a measure of the biosensor sensitivity (Hill coefficient). The K_M value was determined directly from the experimental data while the n value is the best fit to the experimental data using Matlab Curve-Fitting Toolbox and the Hill equation. We estimated from our fitted model, the substrate concentration corresponding to 10% of signal saturation as the lower bound of the linear range of the sensor.

■ ASSOCIATED CONTENT

Supporting Information

Table S1. Table of plasmids. **Table S2**. Table of primers. **Figure S1**. OR1G1- and GPR40-based sensors with P_{Fig1}-GFP multicopy reporter plasmid. **Figure S2**. GPCR-based sensor optimization. **Figure S3**. OR1G1-based sensor performance in a mixture of C14 and C16 fatty acids. **Figure S4**. Fatty acids toxicity to the sensor strains. **Figure S5**. Representative histograms of OR1G1- and GPR40-based sensors with medium chain fatty acids. **Sequences**: OR1G1, GPR40, $P_{Gal4(5x)}$, $P_{LexA(4x)}$, STF1, STF2, G_{olf}. The Supporting Information is available free of charge on the ACS Publications website at DOI: 10.1021/sb500365m.

■ AUTHOR INFORMATION

Corresponding Author

*E-mail: pperalta-yahya@chemistry.gatech.edu.

Author Contributions

P.P.-Y. conceived the project. P.P.-Y., K.M. and S.B. designed the experiments. K.M. and S.B. performed the experiments. P.P.-Y., K.M. and S.B analyzed the data. P.P.-Y., K.M and S.B. wrote the manuscript.

Notes

The authors declare no competing financial interest.

■ ACKNOWLEDGMENTS

This research was supported by Georgia Institute of Technology Start-Up funds, a DARPA Young Investigator Award, and a DuPont Young Professor Award (to P.P.-Y.). The authors thank Prof. Francesca Storici for plasmids.

■ REFERENCES

(1) Wang, H. H., Isaacs, F. J., Carr, P. A., Sun, Z. Z., Xu, G., Forest, C. R., and Church, G. M. (2009) Programming cells by multiplex genome engineering and accelerated evolution. *Nature 460*, 894−898.

(2) Wang, H. H., Kim, H., Cong, L., Jeong, J., Bang, D., and Church, G. M. (2012) Genome-scale promoter engineering by coselection MAGE. *Nat. Methods 9*, 591−593.

(3) Michener, J. K., Thodey, K., Liang, J. C., and Smolke, C. D. (2012) Applications of genetically-encoded biosensors for the construction and control of biosynthetic pathways. *Metab. Eng. 14*, 212−222.

(4) Dietrich, J. A., Shis, D. L., Alikhani, A., and Keasling, J. D. (2013) Transcription factor-based screens and synthetic selections for microbial small-molecule biosynthesis. *ACS Synth. Biol. 2*, 47−58.

(5) Okumoto, S. (2012) Quantitative imaging using genetically encoded sensors for small molecules in plants. *Plant J. 70*, 108−117.

(6) Ostermeier, M. (2005) Engineering allosteric protein switches by domain insertion. *Protein Eng., Des. Sel. 18*, 359−364.

(7) Lynch, S. A., and Gallivan, J. P. (2009) A flow cytometry-based screen for synthetic riboswitches. *Nucleic Acids Res. 37*, 184−192.

(8) Sinha, J., Reyes, S. J., and Gallivan, J. P. (2010) Reprogramming bacteria to seek and destroy an herbicide. *Nat. Chem. Biol. 6*, 464−470.

(9) Schwimmer, L. J., Rohatgi, P., Azizi, B., Seley, K. L., and Doyle, D. F. (2004) Creation and discovery of ligand-receptor pairs for transcriptional control with small molecules. *Proc. Natl. Acad. Sci. U. S. A. 101*, 14707−14712.

(10) McLachlan, M. J., Chockalingam, K., Lai, K. C., and Zhao, H. M. (2009) Directed evolution of orthogonal ligand specificity in a single scaffold. *Angew. Chem., Int. Ed. 48*, 7783−7786.

(11) Yang, J., Seo, S. W., Jang, S., Shin, S. I., Lim, C. H., Roh, T. Y., and Jung, G. Y. (2013) Synthetic RNA devices to expedite the evolution of metabolite-producing microbes. *Nat. Commun. 4*, 1413.

(12) Tang, S. Y., Qian, S., Akinterinwa, O., Frei, C. S., Gredell, J. A., and Cirino, P. C. (2013) Screening for enhanced triacetic acid lactone production by recombinant *Escherichia coli* expressing a designed triacetic acid lactone reporter. *J. Am. Chem. Soc. 135*, 10099−10103.

(13) Zhang, F. Z., and Keasling, J. (2011) Biosensors and their applications in microbial metabolic engineering. *Trends Microbiol. 19*, 323−329.

(14) Ninfa, A. J. (2010) Use of two-component signal transduction systems in the construction of synthetic genetic networks. *Curr. Opin. Microbiol. 13*, 240−245.

(15) Reinscheid, R. and Civelli, O. (2005) De-Orphanizing GPCRs and Drug Development, in *The G-Protein-Coupled Receptors Handbook*, (Devi, L. A., Ed.), Humana Press, New York.

(16) Xue, C. Y., Hsueh, Y. P., and Heitman, J. (2008) Magnificent seven: roles of G protein-coupled receptors in extracellular sensing in fungi. *FEMS Microbiol. Rev. 32*, 1010−1032.

(17) Radhika, V., Proikas-Cezanne, T., Jayaraman, M., Onesime, D., Ha, J. H., and Dhanasekaran, D. N. (2007) Chemical sensing of DNT by engineered olfactory yeast strain. *Nat. Chem. Biol. 3*, 325−330.

(18) Erickson, J. P., Wu, J. J., Goddard, J. G., Tigyi, G., Kawanishi, K., Tomei, L. D., and Kiefer, M. C. (1998) Edg-2/Vzg-1 couples to the yeast pheromone response pathway selectively in response to lysophosphatidic acid. *J. Biol. Chem. 273*, 1506−1510.

(19) Minic, J., Persuy, M. A., Godel, E., Aioun, J., Connerton, I., Salesse, R., and Pajot-Augy, E. (2005) Functional expression of olfactory receptors in yeast and development of a bioassay for odorant screening. *FEBS J. 272*, 524−537.

(20) King, K., Dohlman, H. G., Thorner, J., Caron, M. G., and Lefkowitz, R. J. (1990) Control of yeast mating signal transduction by

DOI: 10.1021/sb500365m
ACS Synth. Biol. 2015, 4, 1261−1269

a mammalian beta-2-adrenergic receptor and GS alpha-subunit. *Science 250*, 121−123.
(21) Versele, M., Lemaire, K., and Thevelein, J. M. (2001) Sex and sugar in yeast: two distinct GPCR systems. *EMBO Rep. 2*, 574−579.
(22) Reilander, H., and Weiss, H. M. (1998) Production of G-protein-coupled receptors in yeast. *Curr. Opin. Biotechnol. 9*, 510−517.
(23) Pausch, M. H. (1997) G-protein-coupled receptors in *Saccharomyces cerevisiae*: high-throughput screening assays for drug discovery. *Trends Biotechnol. 15*, 487−494.
(24) O'Malley, M. A., Mancini, J. D., Young, C. L., McCusker, E. C., Raden, D., and Robinson, A. S. (2009) Progress toward heterologous expression of active G-protein-coupled receptors in Saccharomyces cerevisiae: Linking cellular stress response with translocation and trafficking. *Protein Sci. 18*, 2356−2370.
(25) Emmerstorfer, A., Wriessnegger, T., Hirz, M., and Pichler, H. (2014) Overexpression of membrane proteins from higher eukaryotes in yeasts. *Appl. Microbiol. Biotechnol. 98*, 7671−7698.
(26) Fukutani, Y., Hori, A., Tsukada, S., Sato, R., Ishii, J., Kondo, A., Matsunami, H., and Yohda, M. (2015) Improving the odorant sensitivity of olfactory receptor-expressing yeast with accessory proteins. *Anal. Biochem. 471*, 1−8.
(27) Minic, J., Persuy, M. A., Godel, E., Aioun, J., Connerton, I., Salesse, R., and Pajot-Augy, E. (2005) Functional expression of olfactory receptors in yeast and development of a bioassay for odorant screening. *FEBS J. 272*, 524−537.
(28) Peralta-Yahya, P. P., Zhang, F. Z., del Cardayre, S. B., and Keasling, J. D. (2012) Microbial engineering for the production of advanced biofuels. *Nature 488*, 320−328.
(29) Knothe, G. (2009) Improving biodiesel fuel properties by modifying fatty ester composition. *Energy Environ. Sci. 2*, 759−766.
(30) Knothe, G. (2014) A comprehensive evaluation of the cetane numbers of fatty acid methyl esters. *Fuel 119*, 6−13.
(31) Leber, C., and Da Silva, N. A. (2014) Engineering of *Saccharomyces cerevisiae* for the synthesis of short chain fatty acids. *Biotechnol. Bioeng. 111*, 347−358.
(32) Torella, J. P., Ford, T. J., Kim, S. N., Chen, A. M., Way, J. C., and Silver, P. A. (2013) Tailored fatty acid synthesis *via* dynamic control of fatty acid elongation. *Proc. Natl. Acad. Sci. U. S. A. 110*, 11290−11295.
(33) Choi, Y. J., and Lee, S. Y. (2013) Microbial production of short-chain alkanes. *Nature 502*, 571−574.
(34) Zhang, F. Z., Ouellet, M., Batth, T. S., Adams, P. D., Petzold, C. J., Mukhopadhyay, A., and Keasling, J. D. (2012) Enhancing fatty acid production by the expression of the regulatory transcription factor FadR. *Metab. Eng. 14*, 653−660.
(35) Runguphan, W., and Keasling, J. D. (2014) Metabolic engineering of *Saccharomyces cerevisiae* for production of fatty acid-derived biofuels and chemicals. *Metab. Eng. 21*, 103−113.
(36) Erlenbach, I., Kostenis, E., Schmidt, C., Hamdan, F. F., Pausch, M. H., and Wess, J. (2001) Functional expression of M-1, M-3 and M-5 muscarinic acetylcholine receptors in yeast. *J. Neurochem. 77*, 1327−1337.
(37) Dong, S., Rogan, S. C., and Roth, B. L. (2010) Directed molecular evolution of DREADDs: a generic approach to creating next-generation RASSLs. *Nat. Protoc. 5*, 561−573.
(38) Iguchi, Y., Ishii, J., Nakayama, H., Ishikura, A., Izawa, K., Tanaka, T., Ogino, C., and Kondo, A. (2010) Control of signalling properties of human somatostatin receptor subtype-5 by additional signal sequences on its amino-terminus in yeast. *J. Biochem. 147*, 875−884.
(39) Sanz, G., Schlegel, C., Pernollet, J. C., and Briand, L. (2005) Comparison of odorant specificity of two human olfactory receptors from different phylogenetic classes and evidence for antagonism. *Chem. Senses 30*, 69−80.
(40) Itoh, Y., Kawamata, Y., Harada, M., Kobayashi, M., Fujii, R., Fukusumi, S., Ogi, K., Hosoya, M., Tanaka, Y., Uejima, H., Tanaka, H., Maruyama, M., Satoh, R., Okubo, S., Kizawa, H., Komatsu, H., Matsumura, F., Noguchi, Y., Shinobara, T., Hinuma, S., Fujisawa, Y., and Fujino, M. (2003) Free fatty acids regulate insulin secretion from pancreatic beta cells through GPR40. *Nature 422*, 173−176.
(41) Brown, A. J., Dyos, S. L., Whiteway, M. S., White, J. H., Watson, M. A., Marzioch, M., Clare, J. J., Cousens, D. J., Paddon, C., Plumpton, C., Romanos, M. A., and Dowell, S. J. (2000) Functional coupling of mammalian receptors to the yeast mating pathway using novel yeast/mammalian G protein alpha-subunit chimeras. *Yeast 16*, 11−22.
(42) Roberts, C. J., Nelson, B., Marton, M. J., Stoughton, R., Meyer, M. R., Bennett, H. A., He, Y. D. D., Dai, H. Y., Walker, W. L., Hughes, T. R., Tyers, M., Boone, C., and Friend, S. H. (2000) Signaling and circuitry of multiple MAPK pathways revealed by a matrix of global gene expression profiles. *Science 287*, 873−880.
(43) Pi, H. W., Chien, C. T., and Fields, S. (1997) Transcriptional activation upon pheromone stimulation mediated by a small domain of *Saccharomyces cerevisiae* Ste12p. *Mol. Cell. Biol. 17*, 6410−6418.
(44) Golemis, E. A., and Brent, R. (1992) Fused Protein Domains Inhibit DNA-Binding by Lexa. *Mol. Cell. Biol. 12*, 3006−3014.
(45) Peralta-Yahya, P., Carter, B. T., Lin, H. N., Tao, H. Y., and Comish, V. W. (2008) High-Throughput Selection for Cellulase Catalysts Using Chemical Complementation. *J. Am. Chem. Soc. 130*, 17446−17452.
(46) Nehlin, J. O., Carlberg, M., and Ronne, H. (1991) Control of Yeast Gal Genes by Mig1 Repressor - a Transcriptional Cascade in the Glucose Response. *EMBO J. 10*, 3373−3377.
(47) Giaever, G., Chu, A. M., Ni, L., Connelly, C., Riles, L., Veronneau, S., Dow, S., Lucau-Danila, A., Anderson, K., Andre, B., Arkin, A. P., Astromoff, A., El Bakkoury, M., Bangham, R., Benito, R., Brachat, S., Campanaro, S., Curtiss, M., Davis, K., Deutschbauer, A., Entian, K. D., Flaherty, P., Foury, F., Garfinkel, D. J., Gerstein, M., Gotte, D., Guldener, U., Hegemann, J. H., Hempel, S., Herman, Z., Jaramillo, D. F., Kelly, D. E., Kelly, S. L., Kotter, P., LaBonte, D., Lamb, D. C., Lan, N., Liang, H., Liao, H., Liu, L., Luo, C. Y., Lussier, M., Mao, R., Menard, P., Ooi, S. L., Revuelta, J. L., Roberts, C. J., Rose, M., Ross-Macdonald, P., Scherens, B., Schimmack, G., Shafer, B., Shoemaker, D. D., Sookhai-Mahadeo, S., Storms, R. K., Strathern, J. N., Valle, G., Voet, M., Volckaert, G., Wang, C. Y., Ward, T. R., Wilhelmy, J., Winzeler, E. A., Yang, Y. H., Yen, G., Youngman, E., Yu, K. X., Bussey, H., Boeke, J. D., Snyder, M., Philippsen, P., Davis, R. W., and Johnston, M. (2002) Functional profiling of the *Saccharomyces cerevisiae* genome. *Nature 418*, 387−391.
(48) Baba, T., Ara, T., Hasegawa, M., Takai, Y., Okumura, Y., Baba, M., Datsenko, K. A., Tomita, M., Wanner, B. L., and Mori, H. (2006) Construction of *Escherichia coli* K-12 in-frame, single-gene knockout mutants: the Keio collection. *Mol. Syst. Biol.*, DOI: 10.1038/msb4100050.

DOI: 10.1021/sb500365m
ACS Synth. Biol. 2015, 4, 1261−1269